ISSN 2078-6220. Мінералогічний збірник. 2015. № 65. Випуск 1. С. 132–149
Mineralogical Review. 2015. N 65. Issue 1. P. 132–149

UDC 549.5:553.21:553.3.071(477.87)

SIGNS AND PROOFS OF THE QUARTZ FORMATION FROM SILICA GEL IN THE GOLD-BEARING VEINS OF BEREHOVE ORE FIELD (TRANSCARPATHIANS)

N. Slovotenko[1], L. Skakun[1], R. Serkiz[2]

[1]*Ivan Franko National University of Lviv,*
4, Hrushevskyi St.,79005 Lviv, Ukraine
E-mail: nslovotenko@gmail.com
lzskakun@gmail.com
[2]*Scientific-Technical and Educational Centre of Low Temperature Studies,*
Ivan Franko National University of Lviv,
50, Drahomanov St., 79005 Lviv, Ukraine
E-mail: rserkiz@gmail.com

Swingeing majority of the quartz and sulphide-quartz gold-bearing bodies in the epithermal deposits of the Berehove ore field (Transcarpathians, Ukraine) do not carry a structure of successive growth from the walls to the vein centre. The general structural pattern of these veins is usually a homogeneous cryptocrystalline and fine-crystalline quartz array with much less volume percent of druses amount. We attributed these remarkable features to their metasomatic derivation. Hydrothermal quartz from the gold-bearing quartz veins has been analyzed by scanning electron microscope-cathodoluminescence (SEM-CL). The textural features of quartz veins have been described with the emphasis placed upon the mineral relationship, a crystallization sequence, and mainly an inner structure of quartz. Cathodoluminescence imagery revealed numerous unique patterns and helped to determine and interpret physical and chemical processes of the mineral forming. There are evidences of an colloidal origin most of the quartz array. Cryptocrystalline quartz varieties were formed from a silica gel, whereas coarse-crystalline drusy quartz precipitated from solutides. The vein textures of most ore bodies indicate that quartz was formed by metasomatism in the disperse medium, whereas quartz from the sixth ore zone was precipitated from solutides in condition of a crack opening.

Key words: quartz veins, cathodoluminescence, silica gel, Berehove ore field.

Systematic investigations and geological exploration of the Berehove ore field (Transcarpathian region, Ukraine) began in the second part of the 20th century. Berehove ore field contains two deposits: Berehivske and Muzhiyevske, which are the typical low-sulphidation epithermal Au-Ag deposits. Together with similar gold-bearing districts of Slovakia, Hungary, Romania, it belongs to the same metallogenic province of the epithermal gold-bearing deposits [13, 27].

One of the most conspicuous textural features of the gold-bearing veins is the absence of the successive growth features of crystal aggregates from the vein walls to its centre. Only one ore zone (sixth), which is a border between Berehivske and Muzhiyevske deposits, contains textures of consecutive minerals growth patterns. The sixth ore body also shows textures of breaking up and fragmentations of the vein material, which suggests its tectonic origin. All

other ore bodies have no such tectonic characteristics and growth patterns in the free space of opening fissure. The rest of ore zones we consider to form by metasomatic replacement.

The vein mineral assemblages were characterised by using cathodoluminescence (CL). This study investigates the mineralogical, textural, and structural characteristics, which have been studied to constrain the conditions of the formation of the veins. Recently, mane researches paid great attention to the investigations of hydrothermal or metasomatic quartz inner structure by means of CL image analysis [7, 14, 21, 23, 26, 32, 36, 44] often combined with other analytical techniques. The growing interest is also observed in discussion of the colloidal silica role for quartz crystallization at higher temperatures [9, 12, 46] and experimental modelling of systems which can concentrate and transport significant quantities of both silica and ore elements [17]. Colloform quartz is the feature that has the greatest predictive power for distinguishing between ore grade and sub-economic samples [22, 25].

The CL imagenary method gives us the opportunity to interpret the quartz texture as a result of the metasomatic substitution of the carbonate veins and precipitation from the silica colloid. Hypogen silicic alteration of dolomite was described in [22].

A major aim of this study is to prove that the main volume of the ore bodies was formed by crystallization from the silica gel, and partly some drusy quartz crystallized from the solutides. We analyzed textural and structural patterns of these veins to contribute adequate genetic interpretations.

Geology and mineralization. The Berehove ore field is situated in the Inner Carpathian arc in the Ukrainian part of the Eastern Carpathians (Fig. 1). Its mineral deposits are related to volcanic rocks and represent epithermal vein deposits. The gold-polymetallic mineralization in the Berehove ore field is related to the acid volcanism with approximate age of 14–12 Ma connected with Sarmatian areal volcanism [13, 20, 27].

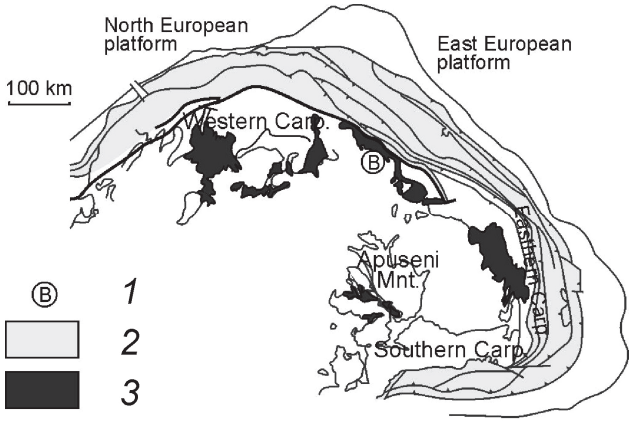

Fig. 1. Location of the Berehove ore field:
1 – Berehove ore field; *2* – Flysch Carpathians; *3* – volcanic rocks (*N*–*Q*).

Stratigraphic profile consists of the three rhyolite thicknesses among which two horizons of the volcanic-sedimentary rocks are situated (Fig. 2). The lower tuffs unit lies directly on the Triassic–Jurassic sediments of the basement. The next thickness of the lower sediment unit covers lower tuffs. These two structural units of the ore field (the Early and Late Badenian) correspond to the precaldera stage of the volcano. The main structural element of the ore field

is the eruptive pipe composed by the middle tuffs units. The middle tuff unit is traced to the depth of 1 500 m. It is represented by psammitic, psephitic, and more rarely by coarse clastic rhyolite tuffs containing fragments of argillite and andesite. The upper sediment unit places mainly over a central zone of the eruptive pipe and is considered to relate to a caldera's lake. The upper sedimentary unit consists of clay, argillite with sandstone and tuff interlayers. Its spread area it is limited by the configuration of the caldera lake. The upper sediment unit is overlapped by the upper tuffs unit, which is composed of the rhyolite tuff, xenotuff, ignimbrite, breccias with tuffite. The two last units correspond to postcaldera volcanic products.

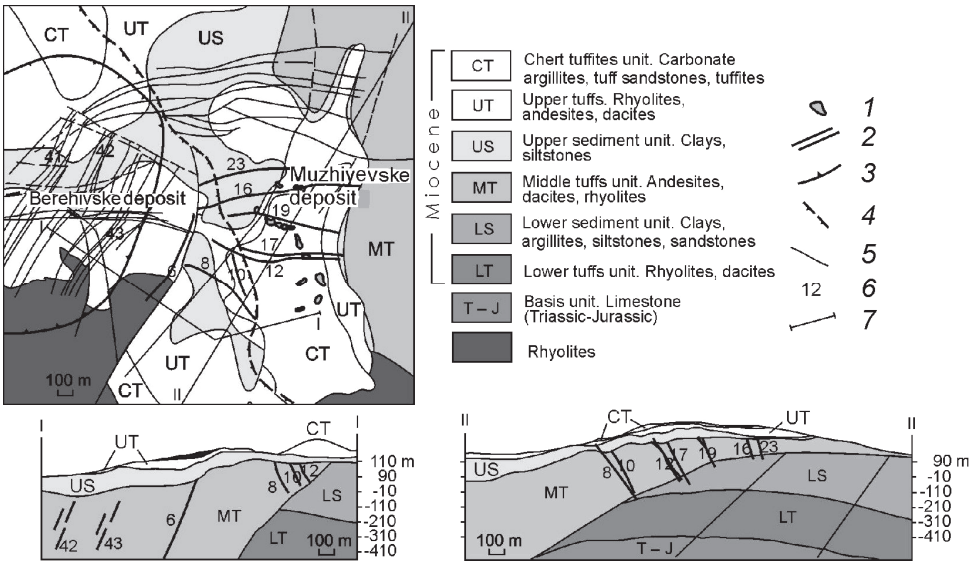

Fig. 2. General geology of the Berehove ore field and individual gold deposits (by the materials of the Transcarpathians Geology Expedition):

1 – stockwork; *2* – ore zones; *3* – caldera fault; *4* – border of the lower sediment unit; *5* – faults; *6* – number of ore bodies; *7* – cross section line.

Ore bodies are represented by veins and stockworks, there are more than fifty ore bodies. Muzhiyeve deposit is located in the inclined part of the Berehove crater and is limited by the north-eastern and eastern shift zone, which runs along the border of the middle and lower sedimentary tuff strata. In the west the deposit is limited by the sixth fracture zone. The Berehove deposit is located in the central part of the eruptive pipe, where there are no lower sedimentary unit and basement rocks. Mineralization of the vein type extends to a considerable depth interval over 500 m, ore bodies represented by 41st, 42nd, 43rd ore zones, most of which are found below the horizon +10. It is overlapped by the thick upper sedimentary layer. In the sixth ore zone, which occupies an intermediate position between two deposits, ore bodies occur from horizon +170 m to horizon –700 m. The sixth ore zone is a fault disorder of the submeridional strike of a curved (in plan) form in the inner part of the caldera.

The vein system consists of several high-angle quartz veins that extend almost vertically from 100 m to more than 300 m, filling a conjugate system of north-eastern or western and north-western spread strike-slip faults connected with wall caldera contraction within the eruptive pipe. Due to contraction, subsidence of the central part of the pipe took place with ampli-

tude of 100 to 180 m. The subsidence led to the formation of joint faults system northeast (6^{th} and 10^{th} fault zones) and a sublatitudinal western and north-western (8^{th}, 12^{th}, 15^{th}, 16^{th}, 19^{th}, 23^{rd} fault zones) stretch. These fault zones are located exclusively in the middle tuff unit and the upper sedimentary unit. The sulphide, quartz-sulphide, quartz-barite, quartz-goethite, quartz veins, and veinlet zones are associated with these fracture zones. The host rocks are the middle tuff unit. The ore veins of sulphide, quartz-sulphide, barite-quartz, and quartz composition are connected with the fracture zones of western spread. The veins are steeply dipping to subvertical. Stockworks are spread on the highest horizons of the Muzhiyeve deposit. The veins are commonly accompanied by zones of silicification, adularization and sericitization. Alteration on the upper horizons is argillization of a different extent. The veins are confined to a vertical extent of approximately 300 m. They range in thicknesses from first centimetres to 3 m.

The ore bodies have been formed during four stages: sulphide, barite-quartz, carbonate-quartz, and carbonate-goethite [41]. The metasomatic mineralization of the first sulphide stage was imposed on carbonates. The main phase of golden precipitation corresponds to the second barite-quartz stage of the mineral formation. Fluorite, barite, quartz were formed on the second stage. The sequence of filling is the following: gold + chalcopyrite + bournonite + tennantite/tetrahedrite → quartz + barite + fluorite.

Mineral zoning of the barite-quartz stage of mineral formation. Intensity of the quartz development in the Muzhiyevske deposit increases to the north and north-east (Fig. 3), within the separate ore bodies it submits to the structure of filtration zones. The barite mineralization is often developed on the periphery quartz veins in the form of a narrow belt. Across this belt, the intensity of the barite mineralization changes and achieves maximum in the central part (see Fig. 3). A similar regularity we observed in cross section of the quartz-barite veins. The fluorite mineralization is spread in the narrow zone, which contains vein bodies from 17^{th} to 23^{rd} ore zones inclusive. The development of the fluorite mineralization is situated on the upper horizons. The extent of the initial fluorite spreading occupied deep horizons, where there are fluorite relicts replaced by carbonate and quartz.

Analytical methods. The samples include drill-core sections, underground and dumpsite material. All minerals selected were handpicked and checked under a binocular microscope. A standard transmitted light microscopy has been used to examine the thin sections. The photographs of the thin sections were made by the help of a CCD Vision camera joined to the transmitted light microscopy. The backscattered electron (BSE) images were obtained on polished thin-sections by a REMMA 102-02 scanning electron microscope model at the Ivan Franko National University of Lviv.

Cathodoluminescence (CL) microscopy. The cathodoluminescence analysis has been used to distinguish mineral structure in the quartz veins with the aim to understand their formation dynamic. It gave us opportunity to visualize diverse structure patterns and growth zoning within quartz and fluorite, which was invisible by a conventional optical microscopy. The luminescence observed in SEM-CL images strongly depends on operating conditions but can be semiquantitatively classified as CL-black, CL-dark, CL-gray, and CL-bright. The thin sections were coated with a carbon layer and were bombarded with electrons with the energy of 20–40 keV and a beam current of 0.24 mA. The electron beam (4 nm cross section) and the sample were maintained in vacuum conditions of $1.33 \cdot 10^{-8}$ bar. The REMMA 102-02 scanning electron microscope with a CL detector (SEM-CL) was used for black-and-white images of the internal growth and textures of the quartz assemblages.

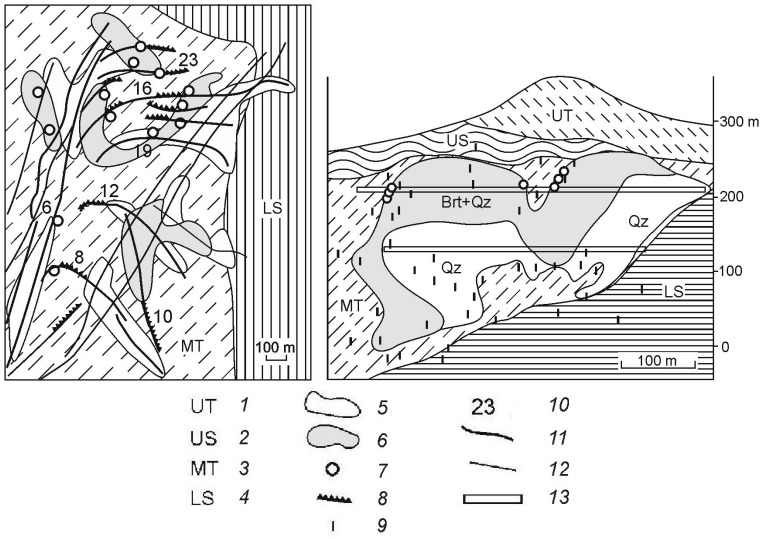

Fig. 3. Spreading of the fluorite-barite-quartz association on the map of horizon +130 and vertical projection of the 19th ore body:

1 – upper tuffs; *2* – upper sedimentary unit; *3* – middle tuffs unit; *4* – lower sedimentary unit; *5–8* – zones of quartz (*5*), barite-quartz (*6*), fluorite (*7*) and sulphides (*8*) development; *9* – intersection of ore body by borehold; *10* – number of ore bodies; *11* – ore zones; *12* – faults; *13* – drifts.

Veins morphology. The shear cracks connected with wall caldera contraction were filled with the carbonates, which subsequently were substituted by the sulphides of the first stage mineralization. Alteration of the older mineralization during the subsequent hydrothermal activity is frequently observed. The carbonates (dolomite, siderite, ankerite, and calcite) are corroded by sulphides, idiomorphic quartz and barite crystals and by aggregates of quartz crystals.

The Au-Ag-bearing veins are of two types: sulphide-quarts and quartz composition. One of the most noticeable textural features of the veins is absence of the successive growth features in the mineral aggregates. Only one ore zone (sixth), which divides Berehivske and Muzhiyevske deposits (see Fig. 2), contains textures of consecutive minerals growth patterns. This ore body also shows textures of breaking up and fragmentations of the vein material, which suggests their tectonic origin. Other ore bodies do not contain any of such tectonic characteristics and growth patterns in the free space of opening fissure from its walls to the centre.

The northern 16th, 19th, and 23rd ore bodies have nearly latitudinal spread; the dip is northern or north-eastern. The ore body thickness varies from 0.05 to 3 m. The contacts of the ore bodies with frame rocks are distinct, nearly vertical. The boundaries are straight or twisted; they are partly complicated with tongues. Sometimes the contacts with country rocks are indistinct because of intensive metasomatic alteration (kaolinization and silification). The elongate clasts of country rock are occasionally included in the veins, generally close to the wall rock contact. Pyrite appears to be the most common sulphide present within the host rock as small crystals. In the veins selvages there are often small fragments of the country rocks, cemented by quartz, sphalerite, and galena.

Quartz is the main mineral in the 15th ore body. The 19th ore body on the deeper horizons consists of quartz with rare barite; on the upper horizons, this ore body changes its character, which becomes compound barite-quartz nature. The 16th ore body is characterized by prevalence of quartz mineralization in close association with barite; sulphide mineralization is spread mainly in one of the selvage parts of this ore body and achieves up to 20 %. The most significant development of the barite-quartz mineralization with fluorite reaches in the 23rd and 12th ore bodies. Sulphide mineralization here is weak. Sulphides are widespread in the sixth ore body. The east flank in the eighth ore body is presented by sulphide mineralization, the western one is fulfilled by quartz and barite. In the 10th ore body sulphides of massive texture dominate, quartz and barite mineralization here is locally developed.

The veins often have sulphide periphery and a quartz centre (Fig. 4). The zones of the vein core are composed of coarse-crystalline quartz. Usually big veins are asymmetrical with sulphides situated in the lying-wall, and quartz settled in the hanging wall. The branches of the veins can be symmetrical with two sulphide selvages. The granular fluorite joins to sulphides aggregates immediately. Its greenish aggregates make units not more than 2 cm. The fluorite positioned not only at the vein edges in contact with rock but is found in quartz mass as separate small grains (up to 3 mm) and octahedral crystals (10–70 μm). Besides the zoned textures in veins there commonly are also massive, symmetric banding, rhythmic banding, colloform, nested, crustiform, and drusy. The banded texture conditioned by the interchange of quartz species and other minerals. The comb textures occur locally, mainly in the middle part of the vein, riming vugs or filling cavities. Fine crustification is widely apparent in the quartz vein. Crustiform colloform quartz textures are abundant.

Sulphides commonly are represented by sphalerite, pyrite, chalcopyrite; galena is less widespread and sulphosalts and marcasite are rare. The sulphide mineralization forms veinlets (their thickness – from 1 to 90 cm), lenses (up to 10–15 cm), small clusters, narrow bands, and scattered fine impregnation in the vein material. Sulphides are more or less oxidized, accompanied with goethite, jarosite, anglesite, and kaolinite.

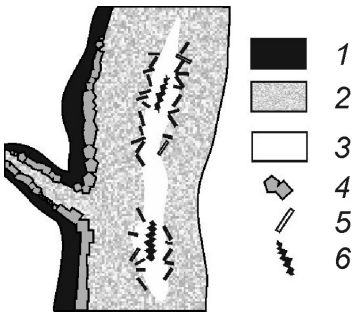

Fig. 4. Morphology of quartz veins: *1* – sulphides; *2* – fine-grained, cryptocrystalline quartz; *3* – coarse-crystalline quartz; *4* – fluorite; *5* – barite; *6* – vug.

Quartz is the main vein mineral, and it displays a range of structures including cryptocrystalline, solid, fine-grained, chalcedony, and drusy species. Very fine-grained and massive cryptocrystalline quartz dominates the vein material. The vein bulk of massive quartz achieves 70 volumetric percent (vol. %), a portion of drusy quartz varies from 0 to 15 vol. %. The size of quartz druses changes from 5 to 10 cm. The individual quartz crystals from these druses reaches 0.5–1.0 cm long. In the voids left after sulphide leaching fine aggregate of the free-flowing quartz appears. The vein quartz is colourless to milk-white. Sometimes vein's quartz tint is reddish or brown because of scattered mineral impregnation of lepidocrocite and goethite, which localizes among grains of the fine-crystalline aggregate. Locally, where the sulphide fine impregnation is sprayed, fine-crystalline quartz is taupe. As a rule, in vugs there are druses of the translucent fine-crystalline quartz. In some vugs, fulfilled with kaolinite, separate, translucent, well faceted quartz crystals with size up to 1 cm (19th ore body) were observed. Amethystine quartz occurs sporadically. Maximum concentrations of gold in quartz vein occur in fine-grained

quartz adjacent to the sulphides. The zones of the vein core composed of coarse-crystalline quartz are generally gold-free or contain minimal gold concentrations.

Tabular barite localized at the central part of vein nearby voids, fulfilled with comb quartz (see Fig. 4). The size of barite crystals varies from shares of millimetre up to five centimetres. In the quartz aggregates, there are sometimes tabular vugs left after the barite leaching. In the sites where dimension of the quartz grains increases, barite crystals become bigger too.

Among rare minerals observed in the ore bodies there are adularia, haematite, jarosite, anglesite, halloysite, manganese oxides.

Signs of the quartz forming from silica gel. ***Microtextures of the quartz veins.*** In thin sections under a microscope there are sites containing structures of recrystallisation of the silica gel, which roughly remind a parquet figure (Fig. 5, *a*). With the lack of such structures in cryptocrystalline quartz in the polarized light only the effect of aggregate polarization is being observed. In the process of recrystallisation the quartz unit dimension of grains has increased, therefore the previous parquet orientation is kept (see Fig. 5, *b*).

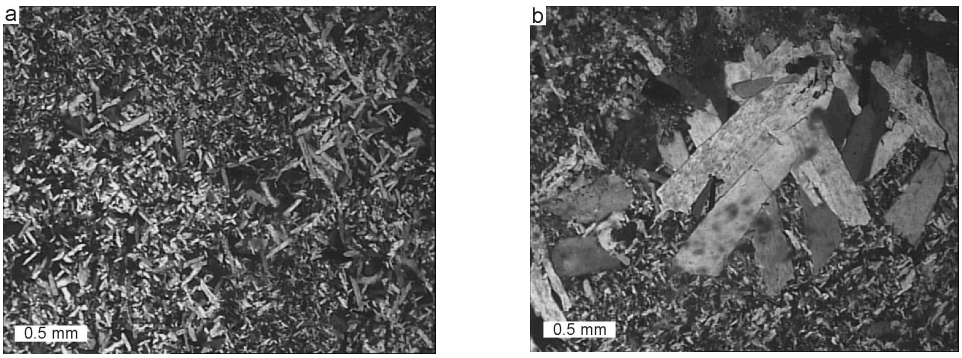

Fig. 5. Quartz structures (polarizing microscope, with analyzer):
a – grains have an oriented parquet figure; *b* – the parquet orientation is kept in the quartz aggregate, which has undergone recrystallisation due to which the grain dimension increased.

Chalcedonic relicts in mineralized veins are frequently – radial-fibrous spherulites and concentric-zone oolites, which are considered to be typical metacolloid feature [5]. The absence of zones of attachment of barite crystals (Fig. 6, *a*) and chalcedonic (see Fig. 6, *b*) or quartz overgrowth around them are characteristic features of veins and proves that barite arises and grows in free medium. The most widespread patterns of barite crystals arrangement are zoned, where they are situated in banded gathering on different angles to one another (Fig. 7, *a*). The less widespread barite structures are represented by framework of the crystals oriented in three directions (Fig. 8). Barite oriented frameworks, as well as quartz structures with parquet orientation, reflect its crystallization in suspended state in the more or less homogeneous environment. As a rule, the fine-grained barite associates with the fine-grained quartz and the coarse-grained barite associates with the coarse-grained barite that testifies about their simultaneous growth and about degree saturation changes in the mineralization environment.

The sticking of the fine gas bubbles to the barite crystal surfaces took place in the quartz aggregates (see Fig. 8, *a*, *b*). The bubbles have a faced appearance. The size of bubbles does not exceed 0.1 mm. The frequency of their sticking is very changeable: some barite crystals are completely surrounded by such bubbles (see Fig. 8, *a*), the others have a single sticking (see Fig. 8, *b*).

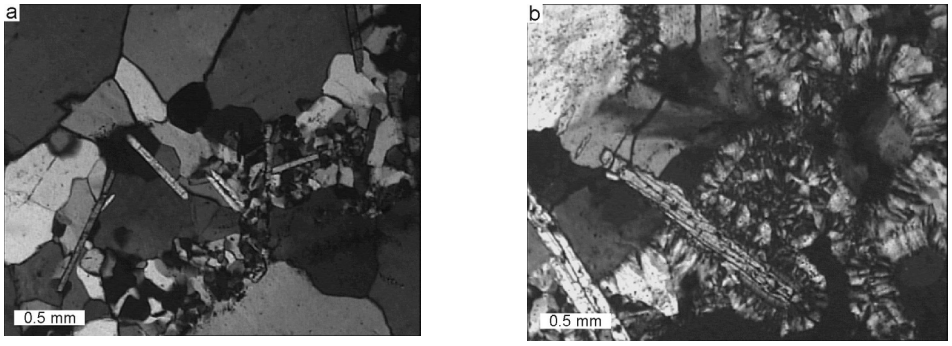

Fig. 6. Barite-quartz aggregate (polarizing microscope, with analyzer):
a – the elongated barite crystals are suspended, they haven't got an any attachment surface; *b* – chalcedonic overgrowth around the barite individual crystals.

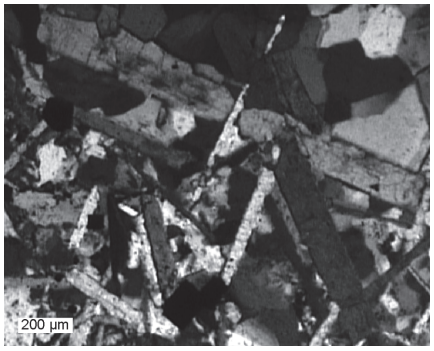

Fig. 7. Barite-quartz aggregate (polarizing microscope, with analyzer). The barite structures are represented by framework of the crystals oriented in three directions.

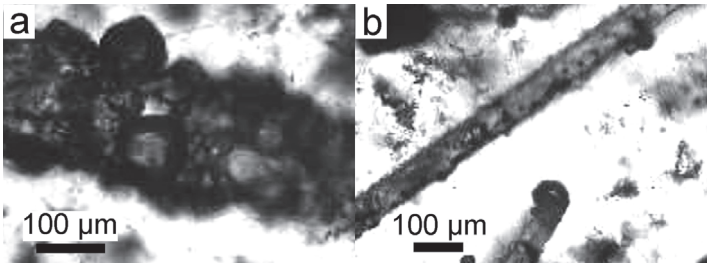

Fig. 8. Gas bubbles sticked on the barite crystal surface in the barite-quartz aggregate.

In some individual cases, the bubbles become a local cause of the barite crystal growth stopping. In some places the point of bubble contact on barite surface was transformed into the pit as free growing sections of quartz partly overgrown the incompatible phase. Such gas bubbles could exist in the viscous gels as open structure of silica gel, which is able to contain big quantity of incompatible contaminants and gaseous matter [9, 19]. During the progressive process of the barite-quartz aggregate maturing incompatible bubbles were partitioned to barite margins.

Scanning electron microscope CL imagery. Cathodoluminescence gave us an opportunity to describe the different morphological varieties of the quartz and their spatial distribution, as well as the morphology and spatial distribution of other minerals, not noticeable under the optical microscopy. Quartz displays variations in intensity of scanning electron microscope-cathodoluminescence (SEM-CL). Microobservations indicate that separate domains with different microstructures exist in the veins. Changes from one to the other structural variety can be gradual or drastic. Thus SEM-CL reveals surprisingly variable textural species of very fine particles quartz aggregates in veins: with patchy, zoned CL nature more or less contrasting to one another (Fig. 9, *a*), drusy aggregates (usually labeled with zoning) (see Fig. 9, *b*, *c*), spotty bands reminding flowers or plumes (see Fig. 9, *d*), or tubes (see Fig. 9, *e*), small flakes with any suggestion of crystal faces (see Fig. 9, *f*). The euhedral to subhedral quartz crystals exhibit dark core with a fine oscillatory growth zoning, and a strong bright CL rim (see Fig. 9, *b*, *c*). The periphery of these rims in bigger crystals is good seen to be splintered (see Fig. 9, *c*). A noteworthy feature of quartz structure revealed by CL is the presence of a considerable amount of isolated zoned and non-zoned quartz crystals (the size is 5 mm or less), which are placed in the massive cryptocrystalline quartz, similarly to porphyritic crystals (see Fig. 9, *g*, *h*). Owing to CL there are noticeably visible innumerable minute blocks in the centre of some of them (see Fig. 9, *g*) and an irregular inner structure (see Fig. 9, *h*).

Syneresis microcracks are often observed in the quartz aggregates (see Fig. 9, *g*), they have no connection with tectonic cracks and are the result of gel ageing [5, 19]. They usually have a twisted morphology and are fulfilled with later quartz. These syneresis microcracks have a later overgrowing of the crustiform fine-grained quartz.

One of the characteristic textures of quartz aggregates is rhythmically zoned, which exhibit arrangement in a regular repeating pattern. Precipitation occurring in a diffusion-controlled gel system often forms reproducible, periodic patterns [3, 15, 24, 30, 31]. In our case, the periodic patterns are presented by the interchange of quartz crystals sizes in bands: from the cryptocrystalline to the fine-crystalline drusy (Fig. 10). The change of the size species between the stratums is drastic. The thicknesses of bands are approximately the same in one level and slightly changeable in different repeating rhythms. The bands characterize by analogous CL brightness on the same level. In some individual rhythms the barite crystals may occur. Usually the barite of the Berehove ore field does not show luminescence.

Noteworthy to admit, that the barite crystals (Fig. 11, *a*) as usual are placed on boundaries where quartz changes its CL characteristics (see Fig. 11, *b*). Such textures appeared on the boundaries, which are dimensionally isolated parts of the different gel viscosity. The division of silica gel into areas of somewhat different degree of polymerization created phase boundaries, which facilitated energy consumption on the formation of barite crystal nucleus.

Let's pay attention to the barite arrangement patterns in the quartz aggregate. Quartz is included in the triangular or another shape interstitial space of the barite crystals, where it grew on barite surfaces and occupied all space (Fig. 12). This arrangement, most likely, shows that barite crystals were originally free swimming in silica colloid. Barite has often ragged borders in contact of quartz due to their subsequent mutual interference.

Similar to quartz, fluorite reveals well-developed growth zoning (Fig. 13) as well as a sector zoning. Often the fluorite crystals have splintered periphery (see Fig. 13). Fluorite has its own facets only on a one side; the growth zoning has been developed under these facets. This is evidently the case where the speed of fluorite crystallization has outstripped the quartz's one.

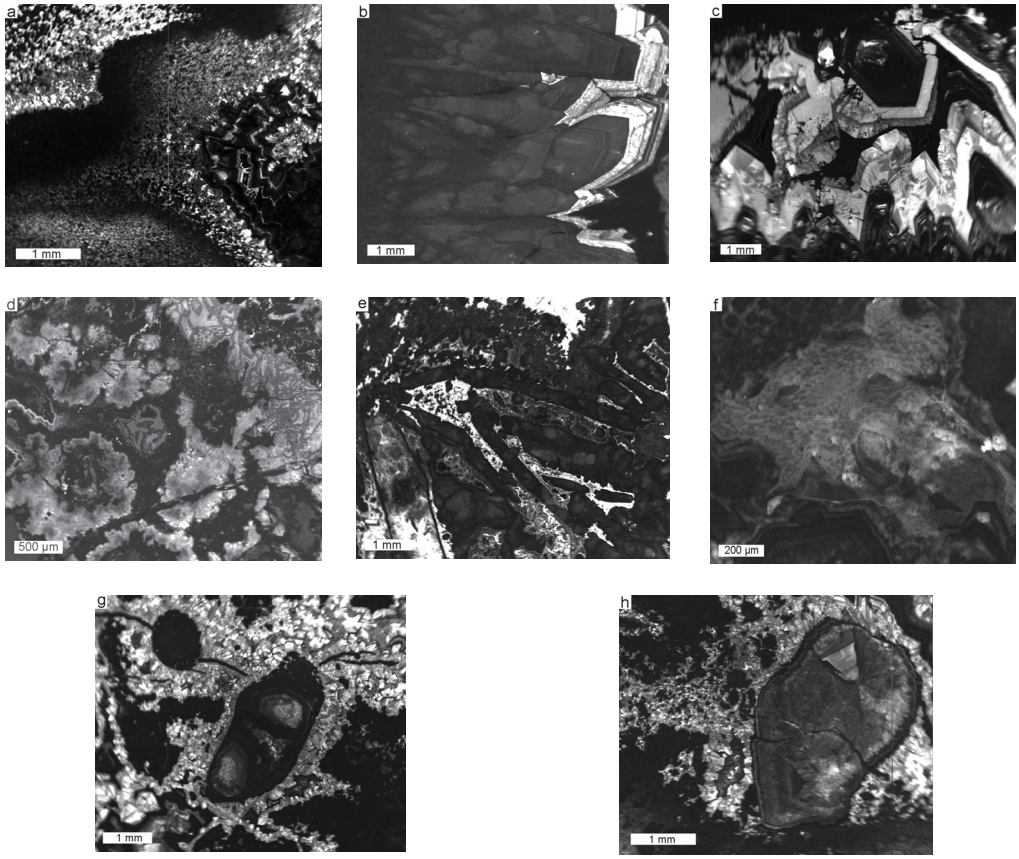

Fig. 9. Scanning electron microscope-cathodoluminescence (SEM-Cl) images reveal the different morphological varieties of the quartz in the veins:

a – zoned aggregate with structure changes from cryptocrystalline to fine-crystalline; *b* – druse quartz, SEM-Cl image reveals a fine oscillatory zoning and a strong bright CL color in the periphery of the aggregate; c – druse aggregate with bright CL-zone in the splintered periphery; *d* – spotty CL bands reminding flowers or plumes; *e* – tubes with a spotty dark CL inside and a bright CL crustification; *f* – small hazy flakes; *g* – separate block crystals of the quartz placed in the array of the cryptocrystalline quartz crustification; there are also roundish black CL aggregate, a syneresis microcrack with the later crustiform fine-grained aggregates; *h* – separate zoned individual crystal with the blocky structure and the later crustiform fine-grained overgrowths.

Therefore, quartz is accrued on the fluorite crystals. Sometimes on its way, fluorite catches barite crystals, which have generated earlier, and partly or completely fills the intervals between them.

The given textural attributes allow us to assert that the formation of the quartz was preceded by the precipitation of amorphous silica from a gel, which has crystallized further in the chalcedony and quartz. Usually, the silica precipitates from geothermal brines as colloidal amorphous silica [2, 4, 9–11, 18, 35, 42–45]. Colloform, spheroidal textures, radial-fibrous spherulites, chalcedonic relicts, syneresis microcracks are considered to be typical metacolloid feature [5, 9, 16, 29, 38]. Periodic patterns structures are usual for diffusion-controlled gel systems [3, 15, 24, 30, 31]. In the most of the hydrothermal system the transformation of the

amorphous precursor to the more thermodynamically stable polymorphs species with low activation energy such as quartz or chalcedony takes place [6, 16].

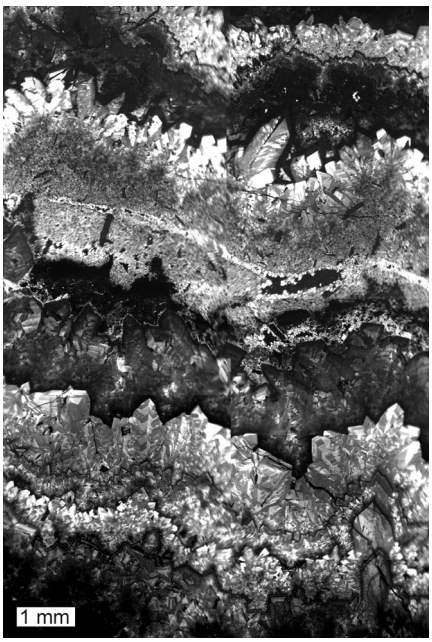

Fig. 10. SEM-CL-image of the rhythmically zoned quartz aggregate.

The image is composed from several smaller. In the middle of the image, there is a zone of the crypto-crystalline quartz, which contains a cavity and syneresis crag healed by later quartz with brighter CL.

The silica gel was non-homogeneous in its volume; it had different degree of thickness and watering. It was divided into separate parts or zones, some of which were more or less stagnant. Prevalence of the cryptocrystalline quartz varieties in the largest vein bulk testifies predominance of the stagnant zones in the crystallization medium. Various conditions of the initial amorphous substratum crystallization had led to the forming of the different aggregation types observed in the veins. Ageing of silica gel had led to the formation of the syneresis cracks; they possibly became conduits for infiltration and solution circulation. The presence of the coarse-crystalline drusy quartz units in the veins reflects existence of the filtration channel for hydrothermal solution in the primary gel matrix. Drusy quartz could form from the solution, which was exuded during syneresis. The local crystallization centres in the overall vein bulk were situated irregularly. The correlation of these different centres had determined origin of the heterogeneous, banded, and zoned mineral unit allocation. Thus, the primary gel medium was heterogeneous. Among different thickness zones there were phase boundaries, which allocated crystal nucleation of the barite and fluorite. Naturally, there is a zoning in quartz assemblages where they are gathered in banded zoned accumulation.

The growth of the barite and fluorite was possible because the gel allowed diffusion of the components necessary for their forming.

Another prominent feature of the heterogeneous gels was the origin in them of semipermeable membranes and penetration of less concentrated solution to the zones with higher concentration because of osmotic pressure. This occasionally causes stretching and rupturing of the membrane [40]. The rejected solution is less dense than the polymerized gel. In such cases so-called chemical gardens are formed [8, 33, 39] in the gel environment. The examples of this process may reflect spotty bands reminding flowers or plumes (see Fig. 9, *d*) and tubular structure (see Fig. 9, *e*) in quartz veins.

Heterogeneous structures that remind a feather or flowers may represent also the coalescence of the coacervated drops in the colloid system. When sour solutions arrive into the sol rapid destruction of solvation spheres of silica micelles and gel forming with next rapid crystallization of gel took place [19], which resulted in forming of these inhomogeneous cryptocrystalline structures with such CL patterns (see Fig. 9, *d*, *f*). Crystallization took place slower in the areas where an electrolyte did not enter. As the result, there are fine-grained aggregates of quartz formed by the mechanism of mass crystallization [28].

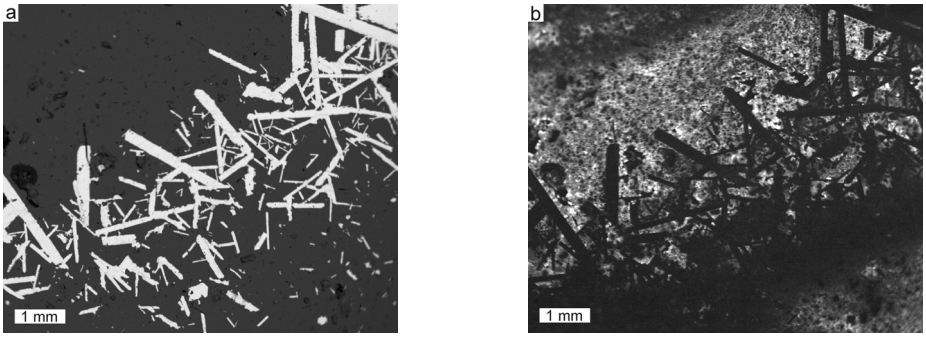

Fig. 11. Barite-quartz aggregate:

a – BSE-image (barite is light, quartz is dark); *b* – SEM-CL-image (it demonstrates that barite zone is situated on the boundary of quarts array with different CL properties).

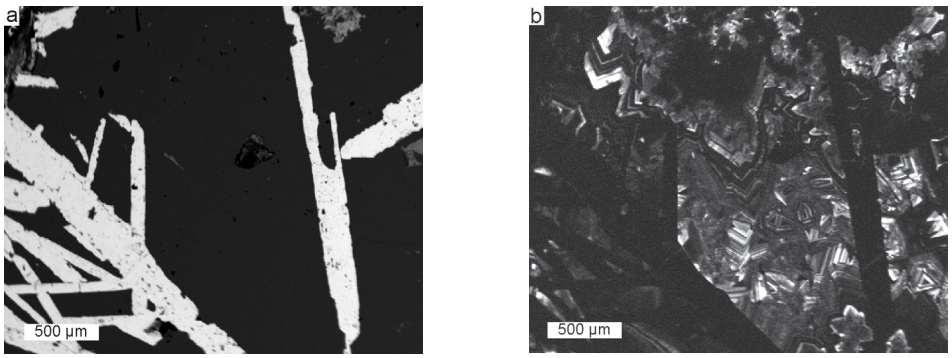

Fig. 12. Barite-quartz aggregate:

a – BSE-image (barite is light, quartz is dark); *b* – SEM-CL-image (reveals the quarts structure and zoning among the barite faces).

In cryptocrystalline groundmass quartz there are some relatively large crystals of quartz (see Fig. 9, *g*, *h*). In the given phenomenon Ostwald ripening can be distinguished [8]. Greatly enlarged "greedy giants" [30, 31] were formed in monodisperse homogeneous sol. According to the large crystals from (see Fig. 9, *g*), in the earlier stages of crystallization these crystals were probably merely aggregates of crypt-crystals. With further development, the individual crystals coalesce to form a single large crystal. In the later stages of development, these features were nearly obliterated, so that only a hazy CL mottling gives a clue as to its former composite character. The formation of well faceted crystals shows us the original features of the crystal growth in gels [5, 15]; the characteristic properties of mechanical interaction of crystals with gel are observed. Gel easily recedes before growing crystals – that provides conditions for their idiomorphic development. Sticking of the gas bubbles to the crystal surface certainly could take place in the gel environment. The gaseous phase impurities were adhered toward barite grain boundaries as barite crystals arose in the silica gel, then after silica gel crystallized into quartz, bubbles acquire a faceted appearance (see Fig. 8, *a*).

The quartz crystal zoning (see Fig. 9, *b*, *c*) represents crystallization conditions in the close system, where accumulation of the trace elements took place eventually.

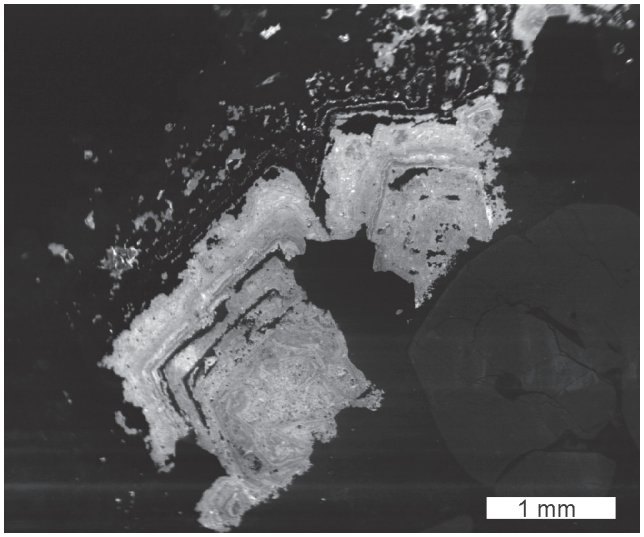

Fig. 13. SEM-CL-image of the fluorite, placed in the quartz aggregate, which here do not show CL. The fluorite crystals are zoned and have the splintered periphery.

First quartz nucleuses do not contain such quantity of the impurities, which have peripheral zones and younger quartz units (see Fig. 9, *b*, *c*). Blocky and splintered inner structure of quartz's rim reflects deformation phenomenon [37], which arise under growth tension in the medium of high viscosity. M. Sander and J. Black [34] described such vein quartz crystals and named them "plumose" quartz.

A frequently observed free-growing barite crystal (see Fig. 6 *a*, *b*, 11, 12) occurred in the viscous environment. The absence of zones of attachment of barite crystals and chalcedonic or quartz overgrowth around them, proves that barite arose and grew freely in the silica gel. Oriented "parquet" quartz structures and barite frameworks arose in the stagnant zones of the gel bulk. Individual crystals there are arranged with minimal quantity of their contacts. The contact of individual barite crystal is dotted only by vertices. The facets of the crystals in solutions are usually blocked by a solvation sphere, which creates a potential barrier to their adhesion. On the vertices the electric double layer is absent, solvate layer thickness is relatively small (0.1 microns or less), so electro-kinetic potential does not prevent sticking [1]. On the tops there are more uncompensated bonds, unlike the faces they possess power of attraction rather than repulsion.

The crystallization of the barite and fluorite promoted quartz crystallization, because it forced the precipitation of the silica gel by the heterogenetic nucleation on their faces. The barite ragged borders in contact with quartz suggest their simultaneous and competitive grow after quartz began to crystallize.

Textural evidence found within the quartz veins, reviled by SEM-CL, does support a former colloidal precursor: the silica colloid, and further gel. The general structural vein patterns suggest that cryptocrystalline quartz varieties were formed from silica gel, whereas coarse-crystalline drusy quartz and metacryst precipitated from solutides.

Barite and fluorite arose in the silica gel environment free swimming; its crystals caused and accelerated the crystallization of the quartz by mechanism of heterogeneous nucleation.

Subsequently these minerals continued to grow simultaneously, which is proved by their ragged competitive borders in contact with the quartz.

We are grateful to the main geologist of Berehove mine V. Drachuk for the help in collecting of mineral specimens and access to the mining documentation.

REFERENCES

1. Askhabov A. M. Processes and mechanisms of the crystallogenesis / A. M. Askhabov. – Leningrad : Nauka, 1984. – 168 p. (in Russian)
2. Bohlmann E. G. Kinetics of silica deposition from simulated geothermal brines / E. G. Bohlmann, R. E. Mesmer, P. Berlinski // Soc. Petrol. Eng. – 1980. – Vol. 20. – P. 239–248.
3. Chadam J. Moving interfaces and their stability: applications to chemical waves and solidification / J. Chadam, P. Ortoleva // Dynamics of Nonlinear Systems. – New York : Gordon and Breach, 1986. – P. 247–278.
4. Chan S. H. A review on solubility and polymerization of silica / Chan S. H. // Geotherm. – 1989. – Vol. 18. – P. 49–56.
5. Chuhrov F. V. Colloids in the Earth's Crust / F. V. Chuhrov. – Moscow : AN SSSR, 1955. – 671 p. (in Russian)
6. Dove P. M. Silica-water interactions / P. M. Dove, J. D. Rimstidt // MSA Rev. Mineral. – 1994. – Vol. 29. – P. 259–308.
7. Evolution of magmatic vapor to gold-rich epithermal liquid: the porphyry to epithermal transition at Nevados de Famatina, Northwest Argentina / C. Pudack, W. E. Halter, C. A. Heinrich, T. Pettke // Econ. Geol. – 2009. – Vol. 104. – P. 449–477.
8. Formation of chemical gardens / J. H. Cartwright, J. M. García-Ruiz, M. L. Novellay, F. Otálora // J. Colloid Interface Sci. – 2002. – N 256. – P. 351–359.
9. Formation of coagulated colloidal silica in high-temperature mineralizing fluids / B. J. Williamson, J. J. Wilkinson, P. F. Luckham, C. J. Stanley // Mineral. Mag. – 2002. – Vol. 66. – P. 547–553.
10. Fournier R. O. Silica minerals as indicators of conditions during gold deposition / R. O. Fournier // US Geol. Surv. Bull. – 1985. – N 1646. – P. 15–26.
11. Fournier R. O. The behavior of silica in hydrothermal solutions / R. O. Fournier // Rev. Econ. Geol. – 1986. – N 2. – P. 45–62.
12. Geochemical constrains from zoned hydrothermal tourmalines on fluid evolution and Sn mineralization: an example from fault breccias at Roache, SW England / B. J. Williamson, J. Spratt, J. T. Adams [et al.] // J. Petrol. – 2000. – Vol. 41. – P. 1439–1453.
13. Geochronology of Neogene magmatism in the Carpathian arc and Intra-Carpathian area / Z. Pécskay, J. Lexa, A. Szakács [et al.] // Geol. Carp. – 2006. – Vol. 57. – P. 511–530.
14. Götze J. Origin, spectral characteristics and practical application of the cathodoluminescence (CL) of quartz – a review / J. Götze, M. Plötze, D. Habermann // Mineral. Petrol. – 2001. – Vol. 71. – P. 225–250.
15. Henish H. K. Crystal Growth in Gels and Liesegang Rings / H. K. Henish. – Cambridge : University Press, 1988. – 198 p.
16. Herrington R. J. Colloidal gold and silica in mesothermal vein system / R. J. Herrington, J. J. Wilkinson // Geol. – 1993. – Vol. 21. – P. 539–542.

17. Hydrosilicate liquids in the system Na_2O–SiO_2–H_2O with NaF, NaCl and Ta: evaluation of their role in ore and mineral formation at high *T* and *P* / S. Z. Smirnov, V. G. Thomas, V. S. Kamenetsky [et al.] // Petrol. – 2012. – Vol. 20. – P. 271–285.
18. Hydrothermal vent fluids, siliceous hydrothermal deposits, and hydrothermally altered sediments in Yellowstone Lake / W. C. Shanks, L. A. Morgan, L. Balistrieri, J. C. Alt // Geothermal Biology and Geochemistry in Yellowstone National Park: Proceeding of the Thermal Biology Institute Workshop, Yellowstone National Park. – WY : Hardcover, 2003. – P. 53–72.
19. Iler R. K. The Chemistry of Silica / R. K. Iler. – New York : John Wiley and Sons, 1979. – 866 p.
20. Koptyuh Yu. M. Gold-Polymetallic Mineralization in the Inner-Carpathian Volcanic Belt / Yu. M. Koptyuh. – Kiev : Naukova dumka, 1992. – 146 p. (in Russian)
21. Landtwing M. R. Relationships between SEM-cathodoluminescence response and trace-element composition of hydrothermal vein quartz / M. R. Landtwing, T. Pettke // Am. Mineral. – 2005. – Vol. 90. – P. 122–131.
22. Lovering T. G. Jasperoids of Pando area, Eagle County, Colorado / T. G. Lovering, A. V. Heyl // Geol. Surv. Bull. – 1980. – N 1474. – P. 1–36.
23. Magmatic and metasomatic processes during formation of the Nb-Zr-REE deposits Khaldzan Buregte and Tsakhir (Mongolian Altai): Indications from a combined CL-SEM study / U. Kempe, J. Goètze, S. Dandar, D. Habermann // Mineral. Mag. – 1999. – Vol. 63. – P. 165–177.
24. Merino E. Survey of geochemical self-patterning phenomena / E. Merino // Chemical Instabilities. – Dordrecht : D. Reidel Publishing Company, 1984. – P. 305–328.
25. Mineral textures and fluid inclusion petrography of the epithermal Ag–Au deposits at Guanajuato, Mexico: Application to exploration / D. Moncada, S. Mutchler, A. Nieto [et al.] // J. Geochem. Explor. – 2012. – N 114. – P. 20–30.
26. Müller A. Trace elements and growth patterns in quartz: a fingerprint of the evolution of the subvolcanic Podlesí Granite System (Krušné hory Mts., Czech Republic) / A. Müller, A. Kronz, K. Breiter // Bull. Czech. Geol. Surv. – 2002. – Vol. 77. – P. 135–145.
27. Neogene-Quaternary volcanic forms in the Carpathian-Pannonian region: a review / J. Lexa, I. Seghedi, K. Németh [et al.] // Cent. Eur. J. Geosci. – 2010. – N 2. – P. 207–270.
28. Nývlt J. Nucleation and growth rate in mass crystallization / J. Nývlt // Prog. Cryst. Growth. Charact. – 1984. – N 9. – P. 335–370.
29. Oehler J. H. Hydrothermal crystallization of silica gel / J. H. Oehler // Geol. Soc. Am. Bull. – 1976. – Vol. 87. – P. 1143–1152.
30. Ortoleva P. J. Solute reaction mediated precipitate patterns in cross gradient free systems / P. J. Ortoleva // Z. Phys. B. Con. Mat. – 1982. – Vol. 49. – P. 149–156.
31. Ortoleva P. J. The self-organization of Liesegang bands and other precipitate patterns / P. J. Ortoleva // Chemical Instabilities: Applications in Chemistry, Engineering, Geology, and Materials Science. – Boston : D. Reidel, 1984. – P. 289–297.
32. Rusk B. Scanning electron microscope-cathodoluminescence analysis of quartz reveals complex growth histories in veins from the Butte porphyry copper deposit, Montana / B. Rusk, M. Reed // Geol. – 2002. – Vol. 30. – P. 727–730.
33. Sainz-Díaz C. I. Microstructures in the formation of chemical gardens / C. I. Sainz-Díaz, J. H. E. Cartwright, B. Escribano // Mater. Res. Soc. Symp. Proc. – 2008. – N 1097. – P. GG07–08.

34. Sander M. V. Crystallization and recrystallization of growth-zoned vein quartz crystals from epithermal systems – implication for fluid inclusion studies / M. V. Sander, J. E. Black // Econ. Geol. – 1988. – Vol. 83. – P. 1052–1060.
35. Saunders J. A. Silica and gold textures in bonanza ores of the Sleeper deposit, Humboldt county, Nevada: evidence for colloids and implications for epithermal ore-forming processes / J. A. Saunders // Econ. Geol. – 1994. – Vol. 89. – P. 628–638.
36. Schmidt Mumma A. Diagenesis and fluid mobilisation during the evolution of the North German Basin – evidence from fluid inclusion and sulphur isotope analysis / A. Schmidt Mumma, M. Wolfgramm // Mar. Pet. Geol. – 2002. – Vol. 19. – P. 229–246.
37. Shtukenberg A. G. Optical Anomalies in Crystals / A. G. Shtukenberg, Yu. O. Punin. – St. Petersburg : Nauka, 2004. – 264 p. (in Russian)
38. Spycher N. F. Evolution of a Broadlands-type epithermal ore fluid along alternative *P-T* paths: implications for the transport and deposition of base, precious, and volatile metals / N. F. Spycher, M. H. Reed // Econ. Geol. – 1989. – Vol. 84. – P. 328–359.
39. Thouvenel-Romans S. Oscillatory growth of silica tubes in chemical gardens / S. Thouvenel-Romans, O. Steinbock // J. Am. Chem. Soc. – 2003. – Vol. 125. – P. 4338–4341.
40. Visual simulation of chemical gardens / Wei X., Qiu F., Li W. [et al.] // IEEE Conf. Publications – Computer Graphics International. – New York : Stony Brook, 2005. – P. 74–81.
41. Vityk M. O. Fluid evolution and mineral formation in the Berehove gold-base metal deposit, Transcarpathia, Ukraine / M. O. Vityk, H. R. Krouse, L. Z. Skakun // Econ. Geol. – 1994. – Vol. 89. – P. 547–565.
42. Weres O. Equations and type curves for predicting the polymerization of amorphous silica in geothermal brines / O. Weres, A. Yee, L. Tsao // Soc. Pet. Eng. J. – 1982. – Vol. 22. – P. 9–15.
43. White D. E. Silica in hot-spring waters / D. E. White, W. W. Brannock, K. J. Murata // Geochem. et Cosmochim. Acta. – 1956. – N 10. – P. 27–59.
44. Wilkinson J. J. Pressure fluctuations, phase separation, and gold precipitarion during seismic fracture propagation / J. J. Wilkinson, J. D. Johnston // Geol. – 1996. – Vol. 24. – P. 395–398.
45. Wilkinson J. J. Silicothermal fluid: a novel medium for mass transport in the lithosphere / J. J. Wilkinson, J. Nolan, A. H. Rankin // Geol. – 1996. – Vol. 24. – P. 1059–1062.
46. Williamson B. J. Formation of coagulated colloidal silica in high-temperature mineralizing fluids / B. J. Williamson, C. J. Stanley, J. J. Wilkinson // Contrib. Mineral. Petrol. – 1997. – Vol. 127. – P. 119–128.

Стаття: надійшла до редакції 28.08.2015
прийнята до друку 04.09.2015

ОЗНАКИ І ДОКАЗИ ФОРМУВАННЯ КВАРЦУ З СИЛІКАГЕЛЮ В ЗОЛОТОНОСНИХ ЖИЛАХ БЕРЕГІВСЬКОГО РУДНОГО ПОЛЯ (ЗАКАРПАТТЯ)

Н. Словотенко[1], Л. Скакун[1], Р. Серкіз[2]

[1]*Львівський національний університет імені Івана Франка,*
вул. Грушевського, 4, 79005 м. Львів, Україна
E-mail: nslovotenko@gmail.com
lzskakun@gmail.com
[2]*Львівський національний університет імені Івана Франка,*
Науково-технічний і навчальний центр низькотемпературних досліджень,
вул. Драгоманова, 50, 70005 м. Львів, Україна
E-mail: rserkiz@gmail.com

У переважній більшості золотоносних кварцових і сульфідно-кварцових рудних тіл епітермальних родовищ Берегівського рудного поля (Закарпаття) не виявлено ознак послідовного наростання від стінок до центра жили. Поширені однорідні прихованокристалічні та дрібнокристалічні, масивні відміни кварцу, які містять незначну кількість друзових агрегатів. Ця особливість свідчить про метасоматичне походження мінералу.

Гідротермальний кварц золото-кварцових жил проаналізовано катодолюмінесцентним аналізом за допомогою сканувального електронного мікроскопа. Текстурні особливості кварцових жил описано з акцентом на мінеральні співвідношення, послідовність кристалізації мінералів та, головно, внутрішню структуру кварцу. За допомогою катодолюмінесцентних зображень виявлено численні унікальні особливості будови жил, визначено й інтерпретовано фізичні та хімічні процеси формування мінералів. Виявлено ознаки колоїдного походження більшої частини кварцу. Прихованокристалічний кварц сформувався з силікагелю, а крупнокристалічний друзовий кварц осаджувався з істинних розчинів. Жильні текстури більшості рудних тіл є доказом того, що кварц утворювався метасоматично в дисперсному середовищі; кварц шостої рудної зони осаджувався з істинних розчинів за умов розкриття тріщин.

Ключові слова: кварцова жила, катодолюмінесценція, силікагель, Берегівське рудне поле, Закарпаття.

ПРИЗНАКИ И ДОКАЗАТЕЛЬСТВА ФОРМИРОВАНИЯ КВАРЦА ИЗ СИЛИКАГЕЛЯ В ЗОЛОТОНОСНЫХ ЖИЛАХ БЕРЕГОВСКОГО РУДНОГО ПОЛЯ (ЗАКАРПАТЬЕ)

Н. Словотенко[1], Л. Скакун[1], Р. Серкиз[2]

[1]*Львовский национальный университет имени Ивана Франко,*
ул. Грушевского, 4, 790005 г. Львов, Украина
E-mail: nslovotenko@gmail.com
lzskakun@gmail.com
[2]*Львовский национальный университет имени Ивана Франко,*
Научно-технический и учебный центр низкотемпературных исследований,
ул. Драгоманова, 50, 79005 г. Львов, Украина
E-mail: rserkiz@gmail.com

В подавляющем большинстве золотоносных кварцевых и сульфидно-кварцевых рудных тел эпитермальных месторождений Береговского рудного поля (Закарпатье) не выявлено признаков последовательного нарастания от стенок до центра жилы. Распространены однородные скрытокристаллические и мелкокристаллические, массивные разновидности кварца, содержащие незначительное количество друзовых агрегатов. Эта особенность свидетельствует о метасоматическом происхождении минерала.

Гидротермальный кварц золотокварцевых жил проанализировано катодолюминесцентным анализом с помощью сканирующего электронного микроскопа. Текстурные особенности кварцевых жил описано с акцентом на минеральные соотношения, последовательность кристаллизации минералов и, главным образом, внутреннюю структуру кварца. С помощью катодолюминесцентных изображений обнаружено многочисленные уникальные особенности строения жил, определено и интерпретировано физические и химические процессы формирования минералов. Выявлено признаки коллоидного происхождения большей части кварца. Скрытокристаллический кварц сформировался из силикагеля, а крупнокристаллический друзовый кварц осаждался из истинных растворов. Жильные текстуры большинства рудных тел являются доказательством того, что кварц образовывался метасоматически в дисперсной среде; кварц шестой рудной зоны осаждался из истинных растворов в условиях раскрытия трещин.

Ключевые слова: кварцевая жила катодолюминесценция, силикагель, Береговское рудное поле, Закарпатье.